

3201.1

72

Library. L. M. A. L.

677



TECHNICAL MEMORANDUMS

NATIONAL ADVISORY COMMITTEE FOR AERONAUTICS

---

No. 797

---

IGNITION PROCESS IN DIESEL ENGINES

By W. Wentzel

Forschung auf dem Gebiete des Ingenieurwesens  
Vol. 6, No. 3, May-June 1935

Washington  
June 1936



NATIONAL ADVISORY COMMITTEE FOR AERONAUTICS

TECHNICAL MEMORANDUM NO. 797

IGNITION PROCESS IN DIESEL ENGINES\*

By W. Wentzel

SUMMARY

The writer analyzes the heating and vaporization process of fuel droplets in a compression-ignition engine on the basis of the theory of similitude - according to which, the period for heating and complete vaporization of the average size fuel drop is only a fraction of the actually observed ignition lag. The result is that ignition takes place in the fuel vapor air mixture rather than on the surface of the drop. The theoretical result is in accord with the experimental observations by Rothrock and Waldron. The combustion shock occurring at lower terminal compression temperature, especially in the combustion of coal-tar oil, is attributable to a simultaneous igniting of a larger fuel-vapor volume formed prior to ignition.

I. INTRODUCTION

The general belief during the first few years following the invention of the Diesel engine - that of Diesel himself included - was that ignition is preceded by vaporization of the fuel. Within the last decade, however, the opinion prevailed that ignition took place on the surface of the drop and that the drop itself burned like the core of coke. This opinion (reference 1) was chiefly based upon Wollers and Ehmke's experiments (reference 2), which disclosed that the oil gases formed by pyrogenic decomposition of the fuels had substantially higher auto-ignition temperatures than the fuels themselves, and upon a theoretical investigation by Neumann (reference 3), according to which the fuel quantity vaporized during the ignition lag was very low.

---

\*"Zum Zündvorgang im Dieselmotor." Forschung auf dem Gebiete des Ingenieurwesens," vol. VI, no. 3, May-June 1935, pp. 105-115.

And now the latest conception is still different (reference 4). The occurrence of an appreciable vaporization of the fuel during ignition lag, is claimed in recent tests by Rothrock and Waldron (references 5 and 6). They photographed the fuel spray in the combustion chamber with a specially constructed apparatus and observed, when no ignition took place, a rapid fogging of the spray after injection, and a clearing during expansion. The investigators attributed this fogging to vaporization and then condensation of the fuel. The observed differences of occurrence under different test conditions speak for the correctness of the explanation.

That the tests by Wollers and Ehmke are no proof of incipient ignition on the liquid fuel, has been shown by Tausz and Schulte (reference 7), who established that the ignition point for fuel vapor formed in the presence of oxygen is the same as for liquid fuel.

Thus the sole remaining proof for the older concept, is Neumann's theory. The rate of vaporization upon which his calculations were based, was established in special tests, in which fuel oil in a tank with large level surface was vaporized under low pressure. But the resulting rate of vaporization is just as little applicable to the vaporization of a droplet as the coefficient of heat transfer during transfer from a flat plate to air is to the case of a small drop or fine wire. Coefficients of heat transfer and vaporization both assume substantially greater values in this case. Since the vaporization factor drops as the pressure rises, the error, committed by applying the vaporization factor established with flat fluid surface to small spheres is, in part canceled for the reason that the fuel in the engine vaporizes at substantially higher density than in Neumann's test tank, so that his theory was bound to yield too small values for the amount of fuel vaporized during ignition lag.\*

---

\*The application of a too low coefficient of heat transfer to the heat transfer from air to the fuel drops, led Neumann in another case (K. Neumann, Z.V.D.I., vol. 76, 1932, p. 765) to erroneous conclusions. Assuming that ignition takes place on the surface of the drops when the latter reaches auto-ignition temperature, he computes from the amount of ignition lag on the basis of a coefficient of heat transfer of  $\alpha = 200 \text{ kcal/m}^2 \text{ h}^0$ , that during the ignition lag itself, material exothermic chemical processes must take place at the surface of the droplets which  
(Continued on p. 3)

## II. CALCULATION OF THE HEATING AND VAPORIZATION PROCESS OF THE FUEL DROP

In the Diesel engine using pressure injection the fuel is sprayed under pump pressure into the air heated by the compression and there atomized. The hot air then transfers heat to the fuel droplets. The fuel starts at the same time to vaporize. Boiling can only occur when the drop reaches the saturation or critical temperature relating to the total pressure in the combustion chamber. With gas oil this does not happen at drop temperatures up to  $350^{\circ}$ , because the pressure at the end of compression is higher than the critical pressure of the proportion of the fuel oil with the highest critical pressure, and the critical temperature of the lowest boiling proportion amounts to about  $350^{\circ}$ . Heating to still higher temperatures is of no interest, because as we shall show, then the drops have almost completely vaporized and the auto-ignition temperature of gas oil at the high density of the combustion air at the end of compression lies far below  $300^{\circ}$ .

For the calculation, it is assumed that the temperature within the fuel drop is immediately compensated; that there is an infinitely large excess of air; that the heat absorption of the fuel oil does not cool the combustion air; and finally, that the fuel-vapor concentration in the remote region surrounding the fuel drop remains zero. These assumptions appear to be closely satisfied for the first sprayed-in fuel drops which decide the amount of the ignition lag.

The following notation is employed:

$r$  (m), radius of droplet.

$r_0$  (m), initial radius of droplet.

---

(Continued from p. 2) accelerate the heating of the drops. On the other hand, the coefficient of heat transfer from air to the spherical droplets is, in absence of any convection  $\alpha = \lambda_L / r$ , where  $r =$  drop radius, and  $\lambda_L =$  air conductivity which, for his assumed  $r = 0.005$  mm drop radius and  $\lambda_L = 0.03$  kcal/m h $^{\circ}$ , gives a value of  $\alpha = 6,000$  kcal/m $^2$  h $^{\circ}$ . At the initially high drop velocities, the heat transfer factor assumes values of  $\alpha > 50,000$ . on the basis of  $\alpha = 6,000$ , Neumann's calculation would make the processes on the drop surface during ignition lag, appreciably endothermic.

$\mu_B$	(kg/mol),	mean molecular weight of fuel vapor.
$\gamma_B$	(kg/m <sup>3</sup> ),	specific weight of fuel.
$c_B$	(kcal/kg <sup>o</sup> ),	specific heat of fuel.
$\rho_B$	(kcal/kg),	heat of vaporization of fuel.
$c_{p_B}$	(kcal/kg <sup>o</sup> ),	specific heat at constant fuel-vapor pressure.
$t$	( <sup>o</sup> C) T ( <sup>o</sup> K),	temperature of fuel droplet.
$\vartheta$	( <sup>o</sup> C) $\theta$ ( <sup>o</sup> K),	temperature in the temperature field around the droplet.
$\vartheta_0$	( <sup>o</sup> C) $\theta_0$ ( <sup>o</sup> K),	constant air temperature in region outside the temperature field surrounding the droplet.
$P_0$	(kg/m <sup>2</sup> ),	total pressure in combustion chamber.
$P_{B_s}$	(kg/m <sup>2</sup> ),	saturation pressure of fuel vapor for temperature $t$ .
$P_{B_0}$	(kg/m <sup>2</sup> ),	partial pressure of fuel vapor in region outside the concentration field surrounding the droplet.
$\alpha$	(kcal/m <sup>2</sup> h <sup>o</sup> ),	coefficient of heat transfer from air to drop.
$\beta$	(m/h),	vaporization factor.
$z$	(h),	time.

The heat absorbed by the drop in time  $dz$  is:

$$dQ = \frac{4}{3} \pi r^3 \gamma_B c_B dt - 4\pi r^2 dr \gamma_B [\rho_B + c_{p_B} (\vartheta_0 - t)] = 4\pi r^2 \alpha (\vartheta_0 - t) dz \quad (1)$$

Thus the quantity of heat absorption includes, besides the growth of the internal energy of the drop and the vaporization heat of the vaporized drop, the heat quantity which serves to heat the oil vapor to the temperature of

the surrounding air. Accordingly,  $\alpha$  includes the pure heat transfer based solely on conductivity and convection (its coefficient is denoted by  $\alpha_w$ ) as well as the heat quantity exchanged by diffusion.

The reduction in weight of the droplet through vaporization is given by

$$-dG = -4\pi r^2 dr \gamma_B = 4\pi r^2 \frac{\mu_B}{848 \theta_m} \beta (P_{B_s} - P_{B_0}) dz \quad (2) \quad *$$

Owing to the high temperature gradient in the concentration field, the partial-pressure difference must be employed in equation (2) (reference 8). For the assumedly infinite excess of air,  $P_{B_0} = 0$ . The partial pressure of fuel vapor on the surface of the droplet is equated to the saturation pressure  $P_{B_s}$  for the respective drop temperature. For vaporization of water the saturation on the surface is less than the saturation concentration according to G. Ackermann (reference 9). No data being available regarding the amount of concentration decrease by the vaporization of oils, it was disregarded.  $\theta_m$  ( $^{\circ}\text{K}$ ) in equation (2) is the mean temperature of the temperature field.

Neglecting the natural convection versus the artificial and assuming high partial fuel pressure but low partial pressure differences, the relationship

$$\frac{\alpha}{\beta} = \frac{\alpha_w}{\beta} = \frac{\lambda_m}{k_m} \left( \frac{\gamma_m c_{p_m} k_m}{\lambda_m} \right)^n \left( 1 - \frac{P_{B_s}}{P_0} \right) \quad (3)$$

exists between  $\alpha$  and  $\beta$  (reference 10):

$\lambda_m$  (kcal/m h $^{\circ}$ ), heat conductivity.

$k_m$  (m $^2$ /h), diffusion coefficient.

$\gamma_m$  (kg/m $^3$ ), specific weight.

$c_{p_m}$  (kcal/kg $^{\circ}$ ), specific heat.

$\alpha_w$  coefficient of pure heat transfer.

---

\*848 in equation (2) is the value of the gas constant (R) for a kg mol when the pressure and volume units are as given.

Subscript  $m$  signifies the integral mean values of the quantities must be taken over the temperature and concentration field. Exponent  $n$  in equation (3) is to be experimentally defined.

However, since in the particular case, both the absolute oil pressures and their differences are great, Ackermann's relation, based upon a boundary layer consideration, must be employed (reference 8) - according to which it is

$$\frac{\alpha}{\beta} = \frac{\lambda_m}{k_m} \left( \frac{\gamma_m c_{pm} k_m}{\lambda_m} \right)^n \frac{P_{Bs} - P_{Bo}}{P_o \ln \frac{P_o - P_{Bo}}{P_o - P_{Bs}}} + \frac{1}{2} c_{pB} \frac{\mu_B}{848 \theta_m} (P_{Bs} - P_{Bo}) \quad (3a)$$

In deriving this equation it was found that - as a close approximation - half the heat quantity necessary for the superheating of the fuel vapor, is solely transported by diffusion, although the same result is obtained for a droplet without convection in the surrounding air.

Equations (2) and (3a) afford:

$$\alpha dz = - dr \gamma_B \left[ \frac{848 \theta_m \lambda_m}{\mu_B P_o k_m} \left( \frac{\gamma_m c_{pm} k_m}{\lambda_m} \right)^n \frac{1}{\ln \frac{P_o - P_{Bo}}{P_o - P_{Bs}}} + \frac{1}{2} c_{pB} \right] \quad (4)$$

which, written in (1) gives:

$$\frac{dr}{r} = \frac{1}{3} c_B \frac{dt}{\rho_B + \frac{1}{2} c_{pB} (\vartheta_o - t) - \frac{848 \theta_m \lambda_m}{\mu_B P_o k_m} \left( \frac{\gamma_m c_{pm} k_m}{\lambda_m} \right)^n \frac{\vartheta_o - t}{\ln \frac{P_o - P_{Bo}}{P_o - P_{Bs}}}} \quad (5)$$

the relation between the drop radius  $r$  and the drop temperature  $t$ . Since  $P_{Bs}$  is a function of  $t$  or, as shown elsewhere, of  $r/r_o$ ,<sup>s</sup> which cannot be expressed as an equation, the integration of (5) is graphically approximated. This has the advantage of ready allowance for the temperature dependence. Visualizing the superheated fuel

vapor as an ideal gas, its heat content  $i_B(\vartheta_0)$  is only dependent on the temperature  $\vartheta_0$ , so that the expression  $\rho_B - \frac{1}{2} c_{pB} (\vartheta_0 - t)$  in (5) may, after introducing the mean specific heats of oil and oil vapor, be written:  $i_B(\vartheta_0) - [c_B]_o^t t - \frac{1}{2} [c_{pB}]_t^{\vartheta_0} (\vartheta_0 - t)$ , and equation (5) becomes:

$$\frac{dr}{r} = dt \frac{\frac{1}{3} c_B(t)}{i_B(\vartheta_0) - [c_B]_o^t t - \frac{1}{2} [c_{pB}]_t^{\vartheta_0} (\vartheta_0 - t) - \frac{848 \theta_m \lambda_m}{\mu_B P_o k_m} \left( \frac{\gamma c_{p_m} k_m}{\lambda_m} \right)^n \frac{\vartheta_0 - t}{\ln \frac{P_o}{P_o - P_{B_s}}} } = dt f(t) \quad (5a)$$

with  $c_B(t)$  as the true specific heat of the fuel oil at temperature  $t$ . The approximate integration of (5a) gives the ratio of the particular drop radius  $r$  to initial radius  $r_o$  versus  $t$ :

$$r/r_0 = F(t) \quad (6)$$

From (6) follows the important fact that, when heating different sized droplets to the same temperature  $t$ , the drop diameter decreases accordingly.

When  $r/r_0$  is known as function of  $t$ , equation (1) may be integrated against the time, but with  $\alpha_w$  rather than heat transfer coefficient  $\alpha$ .  $\alpha_w$  is the coefficient of heat transfer as obtainable by similitude considerations from pure heat transfer experiments on spheres. For pure heat transfer the transferred heat is accordingly about equal to the total heat quantity minus half the excess heat. Equation (1) may also be written:

$$\frac{1}{3} r \gamma_B c_B dt - \gamma_B dr [\rho_B + \frac{1}{2} c_{p_B} (\vartheta_0 - t)] = \alpha_w (\vartheta_0 - t) dz \quad (1a)$$

or

$$\frac{dz}{dz} = \frac{r_0 \gamma_B}{\alpha_w (\vartheta_0 - t)} \left\{ \left( \frac{r}{r_0} \right) \frac{c_B}{3} - \frac{d(r/r_0)}{dt} [\rho_B + \frac{1}{2} c_{p_B} (\vartheta_0 - t)] \right\} dt \quad (1b)$$

Since, unfortunately, no sphere-heat transfer tests have been made,  $\alpha_w$  is expressed as being equal to the value for heat transfer on wires. Ulsamer's equation (reference 11) for it is

$$a_w = \frac{\lambda_m}{2r} 0.536 \left( \frac{2r \gamma_m w}{g \eta_m} \right)^m \quad (7)$$

where  $\eta_m$  = coefficient of viscosity and  $w$  (m/s) = air velocity in undisturbed flow. The exponent  $m = 0.50$  is for Reynolds Numbers of from 50 to 10,000, and  $m = 0.385$  for those between 0.1 and 50. This relation holds true for the inertia condition, which in the case in question does not prevail. Strictly speaking, the time effect (reference 12), which does not appear with the ratio  $\alpha/\beta$ , should be taken into consideration. As this effect is, on the other hand, small at the high initial velocities of the droplet, it may be ignored, and  $\alpha_w$  is, according to (7), dependent upon the momentary speed of the drop. The rate of change of the drop velocity is:

$$- \frac{dw}{dz} = \frac{3}{8} \frac{c}{r} \frac{\gamma_m}{\gamma_B} w^2 \quad (8)$$

where  $c$  is a known function of the Reynolds Number (reference 13). As  $r/r_0$  versus  $t$  is not given as an equa-

tion, and  $\alpha_w$  is a complicated time function, equation (1b) is graphically integrated and becomes, with allowance for the temperature dependence of the specific heat:

$$dz = \frac{r_0 \gamma_B}{\alpha_w (\vartheta_0 - t)} \left\{ \left( \frac{r}{r_0} \right) \frac{c_B(t)}{3} - \frac{d(r/r_0)}{dt} \left[ i_B(\vartheta_0) - [c_B]_0^t t - \frac{1}{2} [c_{p_B}]_t^{\vartheta_0} (\vartheta_0 - t) \right] \right\} dt = \varphi(t, z) dt \quad (1c)$$

$r/r_0$  and  $d(r/r_0)/dt$  being taken from the  $r/r_0 = F(t)$  diagram. The speed after a time interval of  $\Delta z = z_2 - z_1$ , corresponding to an assumed temperature difference of  $t_2 - t_1$  is given by an integration of 8 to

$$w_2 = \frac{1}{\frac{1}{w_1} + \frac{3}{8} \frac{c}{r} \frac{\gamma_m}{\gamma_B} \Delta z} \quad (9)$$

$r$  being expressed as the average drop diameter at  $t_1$  and  $t_2$ , and  $c$  the value for the arithmetic mean of the Reynolds Number for  $z_1$  and  $z_2$ .

For  $w = 0$  speed of drop with no consideration as to the natural convection, the heat transfer coefficient is:

$$\alpha_w = \lambda/r \quad (7a)$$

If  $\alpha_w$  conformal to (7) falls below that of (7a), as occurs at drop rates of less than about  $w = 2$  m/s,  $\alpha_w$  is computed according to (7a).

### III. CALCULATION OF FUNDAMENTAL VALUES

The calculation of the heating and vaporization process was carried out for gas oil.

The specific heat of the fluid gas oil  $c_B$  can, in accordance with Heinlein's experiments (reference 14) be expressed as the linear temperature relationship:

$$c_B = 0.493 + 0.000950 t \quad (10)$$

while, according to Bahlke and Kay (reference 15), the specific heat at constant pressure of the superheated gas-oil vapor follows the linear relation:

$$c_{p_B} = 0.342 + 0.000876 t \quad (11)$$

Heinlein (reference 16) determined the evaporation heat of gas oil at  $t = 170^\circ$  as 63.8 kcal/kg. So assuming that the heat content of the superheated gas-oil vapor depends only on the temperature, we obtain with (10) and (11) the vaporization heat  $\rho_B$  against the temperature of figure 1. Its course compares favorably with the temperature dependence of the heat of vaporization of octane as determined from its vapor-pressure curve (reference 17).

The apparent molecular weight of the gas-oil vapor is put equal to that for tetradecane ( $C_{14} H_{30}$ ) at  $\mu_B = 198$  kg/mol. It corresponds to the average gas-oil composition. The specific weight is given as mean value,  $\gamma_B = 860$  kg/m<sup>3</sup>.

The quantities  $\gamma_m$ ,  $c_{p_m}$ ,  $\lambda_m$ ,  $\eta_m$  represent the integral mean values over the field of temperature and concentration.

Rather than effecting the integration over the concentration range, it was preferred to form the integral mean value over the temperature range for a vapor-air mixture of locally constant vapor concentration equivalent to 50 percent of the temporary concentration on the surface of the droplet. Then

$$\gamma_m = \frac{P_o}{R_m \theta_m} \quad (12)$$

whereby

$$R_m = \frac{848}{\left(1 - \frac{P_{B_s}}{2P_o}\right) \mu_L + \frac{P_{B_s}}{2P_o} \mu_B} \quad (13)$$

and

$$\theta_m = \frac{\theta_o - T}{\ln \frac{\theta_o}{T}} \quad (14)$$

$\mu_L$  is the apparent molecular weight of air.

The specific heat  $c_p$ , on the assumption of a linear temperature relationship for the specific heat of the air, follows from

$$c_{p_m} = \epsilon_L \left[ 0.241 + 0.0000188 \frac{\vartheta_0 + t}{2} \right] + \epsilon_B \left[ 0.342 + 0.000876 \frac{\vartheta_0 + t}{2} \right] \quad (15)$$

the weight fractions of air and fuel vapor being given by

$$\epsilon_L = \frac{\left(1 - \frac{P_{B_s}}{2P_0}\right) \mu_L}{\left(1 - \frac{P_{B_s}}{2P_0}\right) \mu_L + \frac{P_{B_s}}{2P_0} \mu_B}$$

and

$$\epsilon_B = \frac{\frac{P_{B_s}}{2P_0} \mu_B}{\left(1 - \frac{P_{B_s}}{2P_0}\right) \mu_L + \frac{P_{B_s}}{2P_0} \mu_B} \quad (16)$$

The coefficient of heat conductivity of the vapor-air mixture at  $0^\circ$  is:

$$\lambda_0 = \left(1 - \frac{P_{B_s}}{2P_0}\right) \lambda_{L_0} + \frac{P_{B_s}}{2P_0} \lambda_{B_0} \quad (17)$$

and the viscosity is:

$$\eta_0 = \left(1 - \frac{P_{B_s}}{2P_0}\right) \eta_{L_0} + \frac{P_{B_s}}{2P_0} \eta_{B_0} \quad (18)$$

The heat conduction coefficient of the air at  $0^\circ$  is  $\lambda_{L_0} = 0.0209$  kcal/m h $^\circ$ , and the viscosity coefficient  $\eta_{L_0} = 1.69 \times 10^{-6}$  kg s/m $^2$ . The heat conductivity and viscosity factor of gas-oil vapor or its constituents being unknown, we use the values determined for those paraffins having the highest molecular weight: heptane (C $_7$ H $_{16}$ ) =

0.0072 kcal/m h<sup>o</sup>; for heat conductivity and butane (C<sub>4</sub>H<sub>10</sub>) = 0.70 × 10<sup>-6</sup> kg s/m<sup>2</sup> for viscosity factor (reference 18). The temperature relation in both cases is as that of the air. As both λ<sub>B<sub>0</sub></sub> and η<sub>B<sub>0</sub></sub> in (17) and (18) appear multiplied by comparatively small volume proportions of vapor, the error incurred with this simplification is slight. The λ<sub>m</sub> and η<sub>m</sub> values for the drop temperature T follow from

$$\lambda_m = \frac{\lambda_0}{\theta_0 - T} \int_T^{\theta_0} \left(\frac{\theta}{273}\right)^{0.81} d\theta \quad (19)$$

and

$$\eta_m = \frac{\eta_0}{\theta_0 - T} \int_T^{\theta_0} \left(\frac{\theta}{273}\right)^{0.765} d\theta \quad (20)$$

λ<sub>0</sub> and η<sub>0</sub> being given with (17) and (18).

Heinlein (reference 19) determined the diffusion factor of gas oil by measuring an evaporating oil quantity. This method is admissible, provided the vapor-pressure curve is exactly known. According to Heinlein's experiments (reference 20), the vapor-pressure curve of gas oil is dependent upon the size of the container utilized, hence is affected by the oil quantity evaporated. As a result his figures are doubtful. In point of fact, owing to the uncertainty of the vapor-pressure curve, any direct determination of the diffusion factor of binary mixtures, such as gas oil, is probably altogether impossible. The value of each individual constituent must be ascertained.

Gas oil consists chiefly of the paraffins between C<sub>11</sub>H<sub>24</sub> and C<sub>18</sub>H<sub>38</sub>. After defining the diffusion factor of tetradecane (C<sub>14</sub>H<sub>30</sub>), we assumed that the value for the remaining constituents did not diverge substantially. The vapor-pressure curve for C<sub>14</sub>H<sub>30</sub> is available (reference 21). The diffusion factor was established according to Ackermann's method (reference 9) for water vapor, at three different temperatures in an electric chest or in a gas drying chest. Figure 2 shows the experimental points plotted against the temperature for a pressure of 1 atmosphere absolute. The relationship of the diffusion factor to pressure and temperature for any gas may be closely approximated through an equation of the form of

$$k = \frac{k_0}{p} \left( \frac{\theta}{\theta_0} \right)^x \quad (21)$$

whereby  $k_0$  = diffusion factor at 1 atm., and  $\theta_0$  °K,  $p$  = pressure in atm. and  $x$ , a constant about equal to 2. The test data are closely reproducible by the relation (see fig. 2):

$$k = \frac{0.0144}{p} \left( \frac{\theta}{273} \right)^2 \quad (21a)$$

Exponent  $n$  in equations (3) and (5a) is the exponent of  $\frac{c_{pm} \rho \eta_m}{\lambda_m}$  for pure heat transfer; it is put at  $n = 0.31$ , according to Ulsamer's figure for heat transfer of wires (reference 11).

There remains then the saturation pressure  $P_{B_s}$  for the particular temperature of the droplet. The vapor-pressure curve of gas oil is, as already stated, dependent on the amount of evaporated oil. Heinlein's figures for gas oil follow the curve for  $C_{11}H_{24}$  at low temperatures, but become flatter at higher temperatures. In our particular case we made the assumption that the lowest boiling portion is completely vaporized, and that the vapor pressure of the rest of the oil equals the vapor pressure of the still remaining lowest boiling constituent. The calculation is based on the normal boiling curve for gas oil, shown in figure 3. The vapor-pressure curves of  $C_{11}H_{24}$  to  $C_{18}H_{38}$ , are given in figure 4. The extrapolation to higher pressures - no experimental values being available for pressures in excess of 760 mm Hg - followed the relation:

$$\lg P_{B_s} = \frac{A}{T} + B \quad (22)$$

which is applicable because the specific heats of fluid oil and oil vapor are practically the same. The vapor-pressure curves for gas oil obtained by integration of (5a) at  $\theta_0 = 550^\circ$  and  $\theta_0 = 400^\circ$ , are shown in figure 4.

## IV. VAPORIZATION FOR DIFFERENT DROP SIZES

The integration of equation (5a) was carried out for two assumed conditions of combustion air with incipient fuel injection.

1. For  $\vartheta_0 = 550^\circ$  and  $p_0 = 34$  atm. abs., which is about equivalent to the condition of the combustion air at the end of the compression ( $\epsilon = 14$ ).

2. For an air condition which prevails when, with identical compression ratio, as a result of marked wall effect, as occurs when starting the engine, the terminal temperature of the compression stroke attains but  $400^\circ$ ; then the terminal pressure is  $p_0 = 27.8$  atm. abs.

The initial temperature of the injected oil was assumed to be  $t_0 = 20^\circ$ .

Figure 5 shows for both cases the ratio of momentary to original drop diameter  $r/r_0$ , as well as the weight decrease  $\frac{\Delta G}{G_0} = 1 - \left(\frac{r}{r_0}\right)^3$  plotted against the momentary drop temperature  $t$ . There is no perceptible evaporation below  $t = 150^\circ$ , but then it rises very quickly as the drop temperature increases.  $\Delta G/G_0$  is, as already stated, unaffected by the initial drop diameter. The oil volume (in the second case,  $\vartheta_0 = 400^\circ$ ) vaporized during heating to a certain temperature  $t$ , is nearly twice that of the other case ( $\vartheta_0 = 550^\circ$ ). During the longer heating period at low air temperature, the vaporizing quantity is greater than at high temperature. The higher diffusion factor due to lower pressure  $p_0$ , in case 2, is also of influence.

The auto-ignition temperature of gas oil at Diesel terminal compression density is about  $200^\circ$ , according to Tausz and Schulte (reference 7). The proportion of  $\Delta G/G_0$  vaporized while the drop is heated to  $t = 200^\circ$  is quite small; according to figure 5, 2.5 percent in the first, and 5 percent in the second case. However, since according to Tausz and Schulte, the ignition points of liquid fuel and the oil vapors formed in the presence of oxygen are equal, aside from the fact that the auto-ignition temperature of fuel vapor is, according to Tizard (reference 22),

unaffected by the proportion of vapor in the air, it is more likely that ignition takes place in the vapor-air mixture, whose temperature is substantially higher than the auto-ignition temperature, or even in the higher vapor concentration enveloping the drop, rather than on the surface of the drop itself.

The proof for the decisive influence of vaporization during ignition lag, lies with the heating and vaporizing periods obtained by integrating (1c) on the basis of drop diameter  $r_0 = 0.005$  mm for case 1, and  $r_0 = 0.025$  mm for case 2, at an initial drop velocity of  $w_0 = 200$  m/s.

Figure 6 shows the drop temperature  $t$  and the weight decrease  $\Delta G/G_0$  against the time for  $r_0 = 0.005$  mm at  $\vartheta_0 = 550^\circ$  and  $\vartheta_0 = 400^\circ$ . The temperature  $t = 300^\circ$ , in case 1, is reached after 0.00017 second; in case 2, after 0.00055 second. Aside from a brief initial interval, the vaporized quota  $\Delta G/G_0$  rises nearly proportional to the time rate. The vaporized proportion for a given interval is greater in case 1, while with equal drop temperature, according to figure 5, the vaporized proportion of case 2 is greater. When no ignition takes place, the drop is completely vaporized after 0.00058 second in case 1, and after 0.00106 second in case 2.

The assumed diameter  $r_0 = 0.005$  mm, is that of the usual drop size for pressure injection under average conditions, according to Sass (reference 1, p. 45). But there are still substantially smaller droplets - the smallest ones on record being about 0.002 mm diameter - which, naturally, heat and vaporize more quickly. The largest diameter is approximately  $r_0 = 0.025$  mm. Its corresponding  $t$  and  $\Delta G/G_0$  are compared with  $r_0 = 0.005$  mm in figure 7 at  $\vartheta_0 = 550^\circ$ . The ratio of heating periods to a temperature  $t$  for the large and small drops, rises from 12 at low  $t$  to 22 at  $t = 300^\circ$ . The drop temperature  $t = 300^\circ$ , is reached after 0.003 second for  $r_0 = 0.025$  mm; it takes longer than 0.01 second to bring the drop to complete vaporization.

It is important to know the absolute amounts of vapor formed for small and large drops within a certain interval. Putting the weight of the drop of  $r_0 = 0.005$  mm  $G_0(r_0=0.005) = 1$ , the  $\Delta G/G_0$  curve in figure 7, gives the amount of vapor formed  $G(r_0=0.005)$  which, multiplied by

$5^3$  for  $r_0 = 0.025$  mm, gives the absolute amount of vapor  $\Delta G(r_0=0.005)$ , shown in figure 7. It is seen that of two simultaneously injected drops, the one of 0.025 mm diameter gives the greater vapor volume for the first interval (0.0002 second), after which the vapor formed by the 0.025 mm drop becomes preponderant despite its slower heating.

## V. IGNITION LAG

By this is meant the time interval from the start of fuel spray to the visible pressure rise through combustion on the indicator card. In personal bomb experiments (reference 23), the ignition lag for gas oil at combustion air density was established at 0.0048 second at  $\vartheta_0 = 550^\circ$ ; it slowly rises to 0.0072 second at  $\vartheta_0 = 400^\circ$ . The ignition lag is thereby unaffected by the injection pressure. These figures are in good agreement with those of other experimentors (reference 23, p. 24). The computed heating and vaporizing intervals of average fuel drops are substantially lower than the ignition lag. The fundamental premise of infinite excess of air is for the present fulfilled for the first injected particles. But the smallest drops, heated and vaporized quickest, are also the first ones to be slowed up in the air, and are overhauled by the succeeding larger drops of greater penetrating power. As a result, the heating and vaporization in the cooled air of higher fuel-vapor concentration, will be markedly slower in the zone of the fuel spray. For the larger droplets which remain at the spray front and for the particles on the spray edge, the premise of infinitely large excess of air is approximately fulfilled. And the quickest vaporization is accordingly to be expected at these places.

The fact that the ignition lag shows such high figures despite the rapid and material vaporization which at least must occur at the spray edges, is attributable to two causes:

The amount of vapor first igniting at the spray edge is small compared to the total fuel spray, and the heat removed from the spray center, where cold fuel keeps on arriving during injection, is considerable. Thus the heat released by combustion is at the time utilized for heating

and vaporization in the spray core, so that the start of the ignition need not appear as pressure rise. The author's own bomb experiments (reference 23, p. 16) confirmed the existence of a retarding action of the subsequently injected particles on the visible ignition start. They disclosed the ignition lag to decrease with decreasing spray period when the spray period is shorter than the ignition lag.

There also is the possibility of a so-called chemical ignition lag accompanying the igniting of the mixture produced by the vaporization, as established by Tizard and Pye (reference 24) through sudden compression when igniting fuel-vapor-air mixture. These experiments prove that the chemical reaction, even at temperatures considerably above the auto-ignition temperature of the mixture, takes a certain time to develop. The ignition lag in Tizard and Pye's tests assumed, at terminal compression temperature slightly above auto-ignition temperature, values up to 0.75 second and dropped quickly with rising terminal compression temperature. At the highest temperature explored, 66°, the ignition lag, the time interval from reaching of terminal compression point to start of pressure rise, still amounted to 0.007 second, whereas the auto-ignition temperature had already been exceeded 0.018 second before dead center. It is therefore quite possible, even at much higher temperature of the vapor-air mixture, that a chemical ignition lag of such proportions occurs as to constitute a considerable portion of the ignition lag in the Diesel engine.

Proof of the existence of "chemical ignition lag" is found in the observations by Rothrock (reference 5). With high terminal compression temperature, ignition did not take place until after several injections, when the amount of fuel spray was very small, despite the existence of favorable physical conditions for rapid ignition, quick heating, and vaporization. This phenomenon can only be explained by a "chemical ignition lag," which is not only affected by the temperature but also, in accordance with the chemical mass-action law, by the fuel-vapor concentration.

The process accompanying the ignition in the Diesel engine is therefore as follows: On leaving the nozzle, the fuel is very quickly atomized. The droplets penetrating the hot air, are heated and vaporized; the particles on the spray edge and the large droplets on the spray tip encounter the most beneficial conditions, while the process

in the spray core is slowed up by the continued injection of fuel as a result of cooling. Ignition in the forming vapor-air mixture, takes place at the spray edge after termination of the "chemical ignition lag." The first ignition is not visible on the indicator card owing to the heat extracted by the spray core.

With these deductions, further observations of combustion experiments of compressorless oil sprays can be readily interpreted.

Figures 8 and 9 show the author's (reference 23) pressure curve as recorded in the bomb with gas-oil injection at combustion air temperatures before injection, for  $\vartheta_0 = 467^\circ$  and  $\vartheta_0 = 309^\circ$ . The ignition limit, i.e., the temperature of the combustion air at which no more ignition takes place, lies at around  $290^\circ$ . While for case 1, the 0.0053<sup>second</sup> ignition lag is followed by a continuous pressure rise, this lag in case 2 amounts to 0.061 second, and the combustion is explosive-like. In case 1, the heating and vaporization follows in quick order as a result of the high air temperature, the "chemical ignition lag," is short; the amount of fuel injected up to the moment of ignition and the amount of vapor are small. Combustion takes place quickly but mildly. In case 2, the droplet is heated much more slowly, but a relatively large amount of vapor is formed, according to figure 5. The "chemical ignition lag" is great at the low temperature; the marked cooling through the great amount of fuel injected during the long ignition lag prevents the incipient ignition from being visible as pressure rise. The succeeding sudden combustion cannot be visualized in a combustion of fluid particles; it can only be explained on the assumption of the almost completely vaporized fuel at the beginning of the pressure rise.

In figures 10 and 11 we compare the pressure-time diagrams at  $\vartheta_0 = 760^\circ$  and  $\vartheta_0 = 533^\circ$  for the combustion of coal dust with compressed-air injection in the bomb (reference 25). The limit of ignition is about  $480^\circ$ . The pressure and time scales are those of figures 8 and 9. By high air temperature the pressure curve for coal-dust combustion (fig. 10) is like that for burning gas oil (fig. 8), but the absolute ignition lag and combustion period figures are higher for the coal dust. At low air temperature, a fundamental difference prevails: The coal dust burns gradually, while the gas oil burns explosive-like.

If the combustion process in the Diesel engine involved fluid fuel droplets, the pressure-time record would have to be as that for coal-dust combustion. The fact that at high temperature - that is, small ignition lag - the pressure curve for gas oil is similar to that for coal dust, must not be interpreted as a combustion of oil droplets. The shape of the pressure curve at high temperature can also be explained by assuming the oil to be vaporized prior to ignition.

The change in shape of figure 8 to that of figure 9 upon decreasing the temperature, is such that with increasing ignition lag the first part of the pressure rise occurs explosive-like so long as the spray period exceeds the ignition lag. This was observed for coal-tar oil even at very high temperature ( $\vartheta_0 = 580^\circ$ ). The explanation for this is as follows: The boiling range of coal-tar oil is substantially lower than of gas oil, with correspondingly quicker evaporation. The auto-ignition temperature, on the other hand, is markedly higher. Thus, when ignition takes place greater volumes of fuels have vaporized than for gas oil, whose almost simultaneous ignition is followed by a combustion shock.

Alt (reference 26) arrived at the conclusion that, if the vaporization were important for the ignition, a fuel would be so much more favorable as its ignition point was above the boiling point, because then the vaporization before ignition had already further progressed. But the very opposite is true. With low ignition point, ignition takes place quickly; so long as only a small amount of oil is vaporized, ignition takes place without shock.

Rothrock and Waldron's observations (reference 6) were to the effect that the combustion by small pre-injection - that is, high combustion air temperature - took place at the spray edges and took a certain time to fill the whole chamber. By greater pre-injection - that is, lower temperature - combustion took place at once in the whole chamber. The recorded indicator cards then disclose a detonation. This result is in best agreement with the author's experiments.

Translation by J. Vanier,  
National Advisory Committee  
for Aeronautics.

## REFERENCES

1. Sass, F.: Kompressorlose Dieselmotoren, p. 13, Berlin, 1929.
2. Wollers, G., and Ehmke, V.: Kruppsche Mh., vol. 2, 1921, p. 1.
3. Hartner-Seberich, R.: Der Zündverzöger bei flüssigen Brennstoffen. VDI-Forschungsheft 299, p. 11, Berlin, 1928.
4. Schäfer, B.: Jb. schiffbautechn. Ges., vol. 33, 1932, p. 181.
5. Rothrock, A. M.: The N.A.C.A. Apparatus for Studying the Formation and Combustion of Fuel Sprays and the Results from Preliminary Tests. T.R. No. 429, N.A.C.A., 1932.
6. Rothrock, A. M., and Waldron, C. D.: Fuel Vaporization and Its Effect on Combustion in a High-Speed Compression-Ignition Engine. T.R. No. 435, N.A.C.A., 1932.
7. Tausz, J., and Schulte, F.: Über Zündpunkte und Verbrennungsvorgänge im Dieselmotor, Halle 1924.
8. Ackermann, G.: Eine neue Theorie des Aspirationspsychrometers. (To be published.)
9. Ackermann, G.: Ing.-Arch., vol. 5, 1934, p. 124.
10. Nusselt, W.: Z.f.a.M.M., vol. 10, 1930, p. 118.
11. Ulsamer, J.: Forschung, vol. 3, 1932, p. 94.
12. Nusselt, W.: Gesundh.-Ing., vol. 38, 1915, p. 477.
13. Ergebnisse der Aerodynamischen Versuchsanstalt zu Göttingen, II. Lieferung, p. 29, München und Berlin, 1923.
14. Heinlein, F.: Motorwagen, 1925, p. 609.
15. Bahlke, W. H., and Kay, W. B.: Ind. Eng'g Chem., vol. 21, 1929, p. 942.

16. Heinlein, F.: Motorwagen, 1926, p. 397.
17. Landolt-Börnstein: Physikalisch-Chemische Tabellen, 5. Aufl., vol. II, p. 1482; Ergänzungsband Iib, p. 1491.
18. Landolt-Börnstein: Physikalisch-Chemische Tabellen, 5. Aufl., Ergänzungsband Iia, p. 137.
19. Heinlein, F.: Motorwagen, 1925, p. 649.
20. Heinlein, F.: Motorwagen, 1926, p. 398.
21. Landolt-Börnstein: Physikalisch-Chemische Tabellen, 5. Aufl., Ergänzungsband I, p. 730.
22. Tizard, H. T.: Proc. N. E. Coast Inst. Eng. and Shipbuilders, May 1921.
23. Wentzel, W.: Der Zünd- und Verbrennungsvorgang im kompressorlosen Dieselmotor. VDI-Forschungsheft 366, Berlin, 1934.
24. Tizard, H. T., and Pye, D. R.: Philos. Mag., vol. 44, 1922, p. 79.
25. Wentzel, W.: Der Zünd- und Verbrennungsvorgang im Kohlenstaubdieselmotor. VDI-Forschungsheft 343, Berlin, 1931.
26. Alt, O.: Z.V.D.I., vol. 67, 1923, p. 686.  
Wartenberg, H. v.: Z.V.D.I., vol. 68, 1924, p. 153.

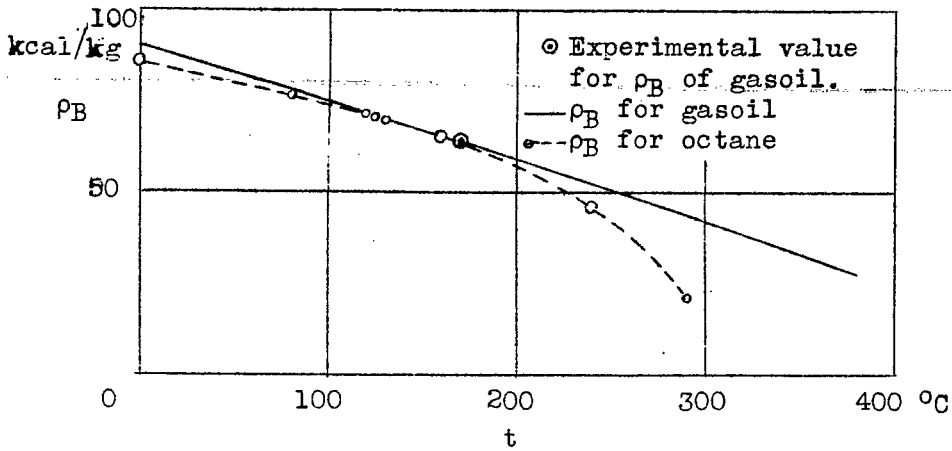


Figure 1.—Computed heat of vaporization  $\rho_B$  of gasoil and octane versus temperature  $t$ .

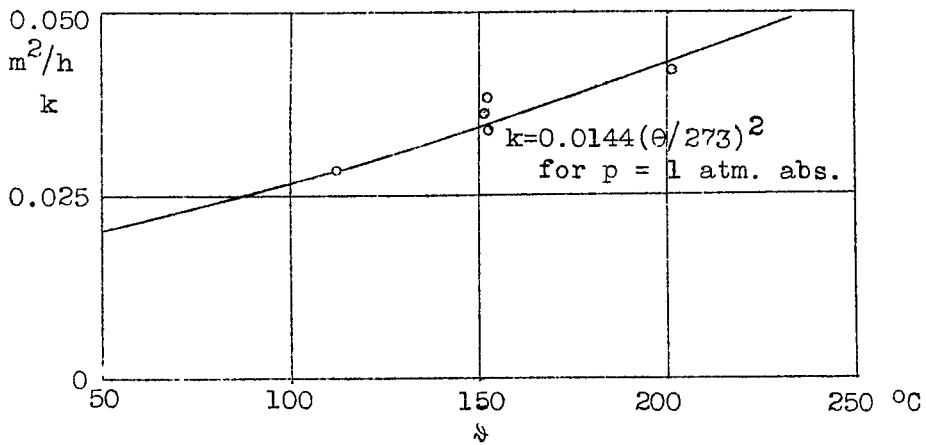


Figure 2.—Diffusion factor  $k$  of tetradecane ( $\text{C}_{14}\text{H}_{30}$ ) against temperature  $t$ .

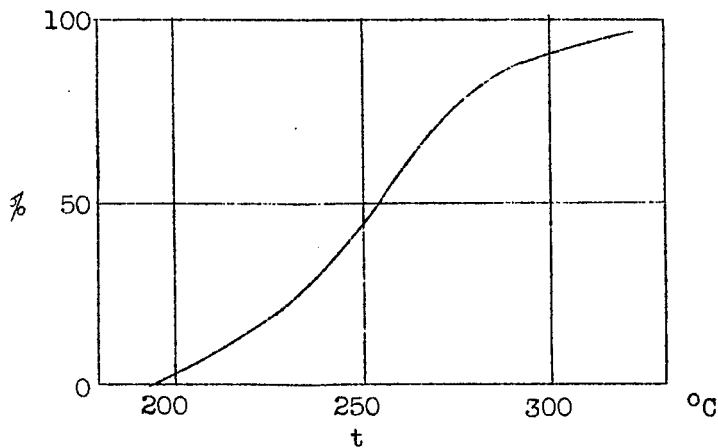


Figure 3.—Boiling curve of gasoil.

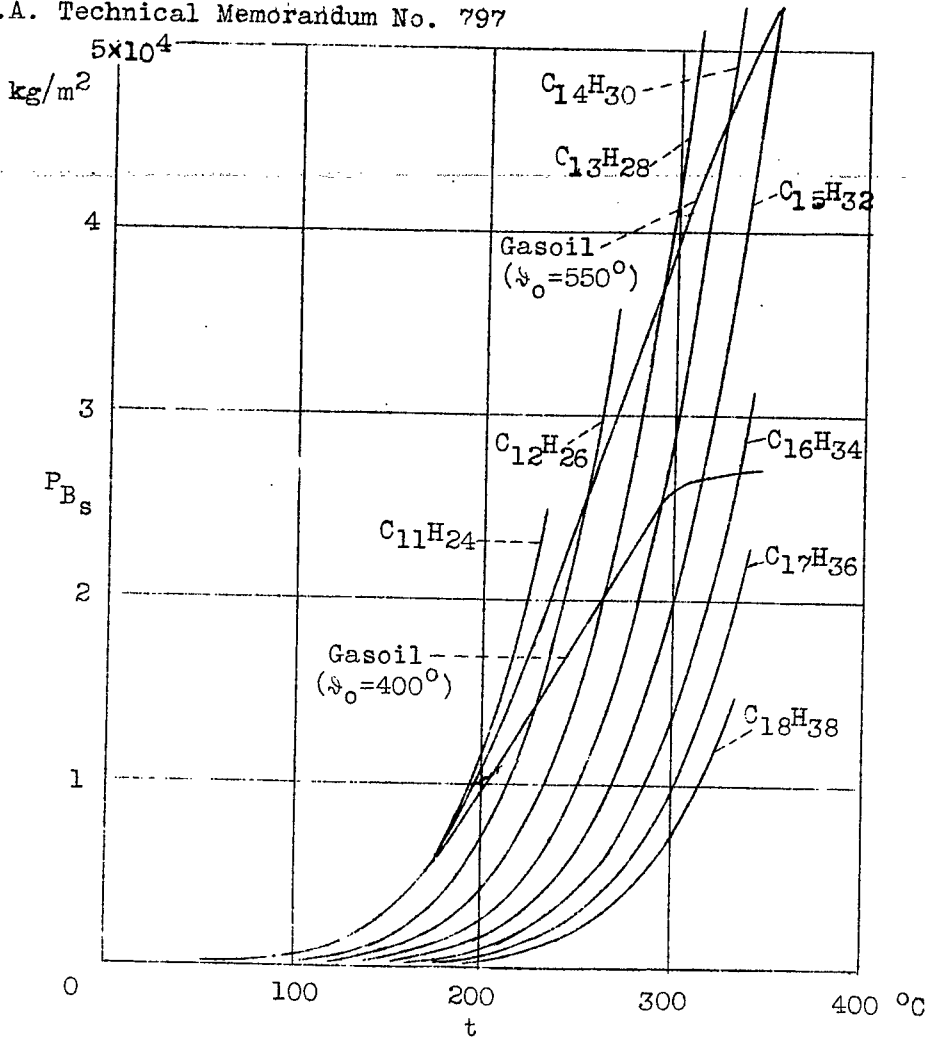


Figure 4.--Vapor pressure for higher paraffines and for gasoil.

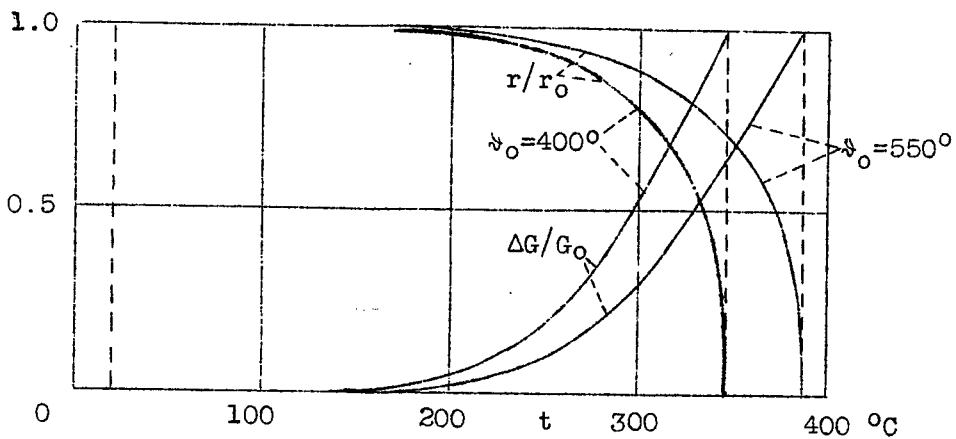


Figure 5.--Ratio of drop diameter  $r/r_0$  and weight decrease  $\Delta G/G_0$  versus drop temperature  $t$  at  $\vartheta_0 = 550^{\circ}$  and  $\vartheta_0 = 400^{\circ}$  air temperature.

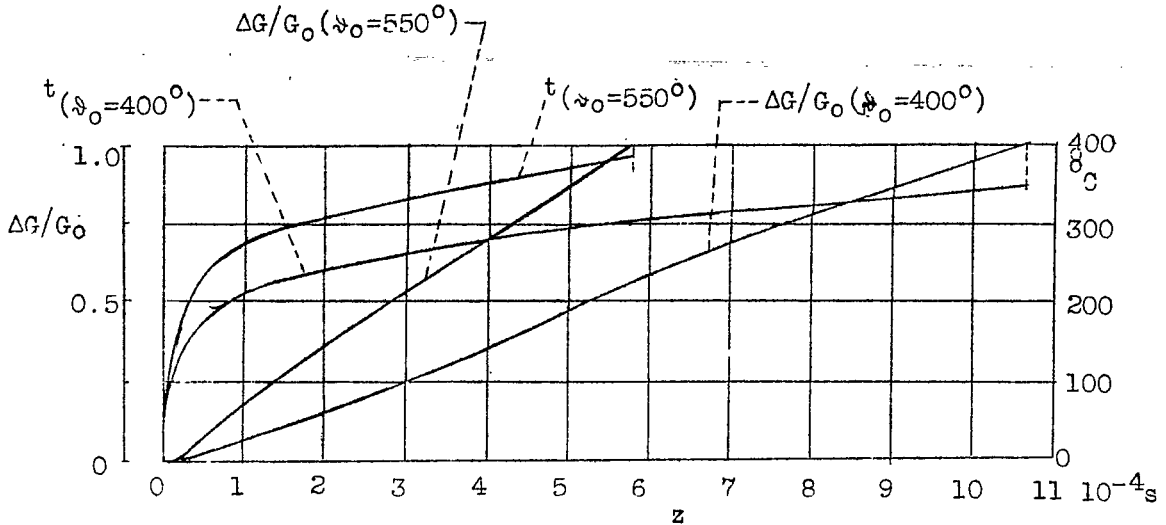


Figure 6.-Drop temperature  $t$  and weight decrease  $\Delta G/G_0$  against time for  $\phi_0=550^\circ$ ,  $p_0=34$  atm. and  $\phi_0=400^\circ$ ,  $p_0=27.8$  atm.,  $r_0=0.005$  mm.

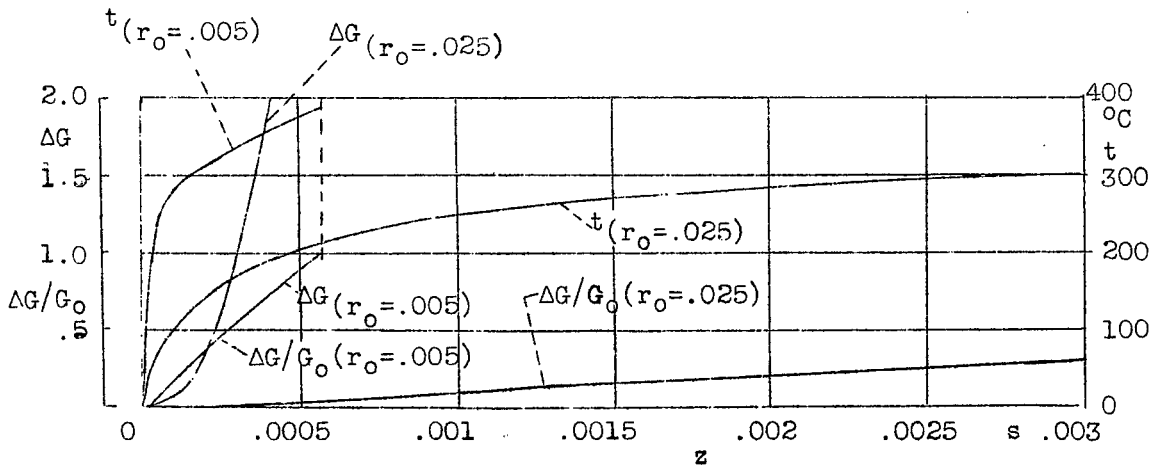


Figure 7.-Drop temperature  $t$ ,  $\Delta G/G_0$  and  $\Delta G$  versus time for  $r_0=.005$  mm. and  $r_0=.025$  mm,  $\phi_0=550^\circ$ ,  $p_0=34$  atm.

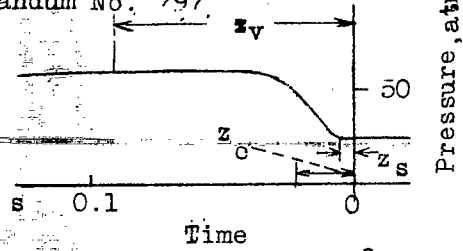


Figure 8.- Gasoil,  $\phi_o = 467^\circ$

$z_e$  = Spray period  
 $z_s$  = Ignition lag  
 $z_v$  = Combustion period

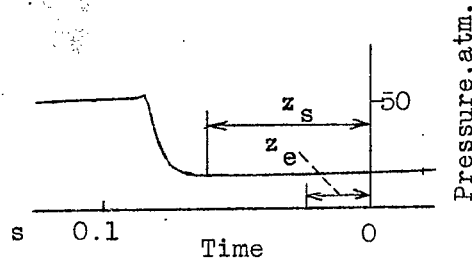


Figure 9.- Gasoil,  $\phi_o = 309^\circ$

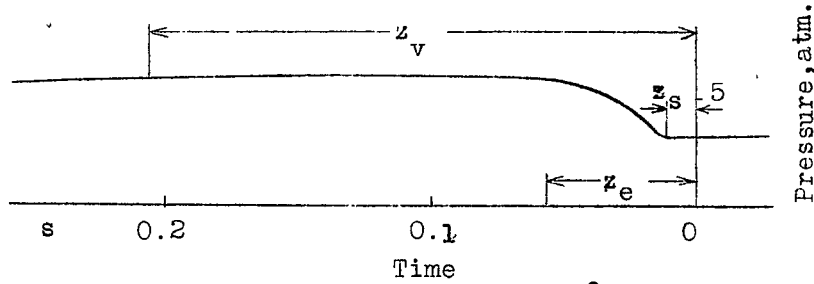


Figure 10.- Coal dust,  $\phi_o = 760^\circ$

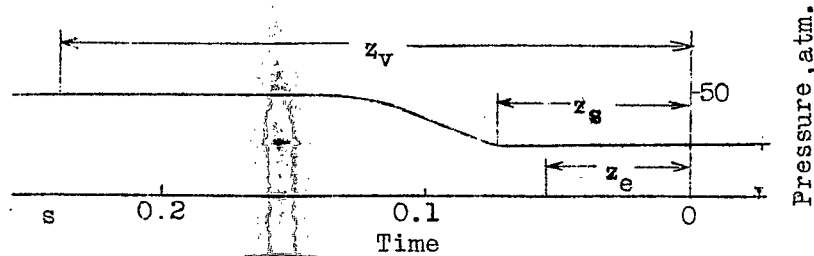


Figure 11.- Coal dust,  $\phi_o = 533^\circ$

Pressure-time record for equal chamber combustion of gas oil and coal dust; air density  $\gamma_L = 10 \text{ kg/m}^3$ .

NASA Technical Library



3 1176 01441 1723